Photochemically induced dynamic nuclear polarization observed by solid-state NMR in a uniformly ^{13}C-isotope labeled photosynthetic reaction center

Shubhajit Paul,[a] *Bela E. Bode,*[b] *Jörg Matysik,*[a] *A. Alia*[c,d]

[a] Universität Leipzig, Institut für Analytische Chemie, Linnéstr. 3, D-04103 Leipzig, Germany

[b] EaStCHEM School of Chemistry, Biomedical Sciences Research Complex and Centre of Magnetic Resonance, University of St Andrews, St Andrews, KY16 9ST, Scotland

[c] Universität Leipzig, Institut für Medizinische Physik und Biophysik, Härtelstr. 16, D-04107 Leipzig, Germany

[d] Gorlaeus Laboratoria, Leiden Institute of Chemistry, Einsteinweg 55, P.O Box 9502, 2300 RA Leiden, The Netherlands

KEYWORDS. Photosynthesis, electron transfer, nuclear polarization, spin diffusion.

ABSTRACT. A sample of solubilized and quinone-depleted reaction centers (RC) from the purple bacterium *Rhodobacter (R.) sphaeroides* wild-type (WT) has been prepared entirely ^{13}C and ^{15}N isotope labelled at all positions of the protein as well as of the cofactors. In this sample, the occurrence of the solid-state photo-CIDNP (photochemically induced dynamic nuclear polarization) effect has been probed by ^{13}C solid-state magic-angle spinning (MAS) NMR under illumination. Under continuous illumination, signal intensities are modified by the three-spin mixing (TSM) mechanism. Time-resolved illumination experiments reveal the occurrence of light-induced nuclear polarization on the time-scale of hundreds of microseconds, initially dominated by the transient polarization of the singlet branch of the radical-pair mechanism (RPM). A first kinetic analysis shows that the lifetime of the polarization from the singlet branch, indicated by the enhanced absorptive intensities of the signals from aliphatic carbons, is significantly extended. Upon arrival of the polarization from the triplet decay branch, emissive polarization caused by the three-spin mixing mechanism (TSM) is observed. Also this arrival is significantly delayed. The decay of TSM polarization occurs in two steps, assigned to intra- and intermolecular spin diffusion.

Introduction

The solid-state photo-CIDNP (photochemically induced dynamic nuclear polarization) effect, discovered by Zysmilich and McDermott in 1994[1], allows for dramatic signal enhancement in solid-state magic-angle spinning (MAS) NMR experiments upon sample illumination (for review, see refs [2,3]). While photo-CIDNP has been observed in the liquid state in various electron-transfer systems, the effect in solid matrix seems to be confined to a few systems: frozen natural photosynthetic systems, where it allows for detailed functional analysis[4,5,6,3,7], as well as a blue-light photoreceptor LOV1-C57S[8,9]. Since all natural photosynthetic systems tested have shown the effect, it has been proposed that the solid-state photo-CIDNP effect is related to the unsurpassed efficiency of natural photosynthetic electron transfer[10]. In solution state, the effect is explained by the well-known radical-pair mechanism[11,12] in which spin-sorting, controlled by nuclear spin states, controls the fate of the reaction dynamics, leading either to recombination or escape products, which can be well distinguished by liquid-state NMR due to different chemical shifts. In the solid state, the radical-pair mechanism can only be observed transiently in time-resolved experiments[13,14] while under continuous illumination, the contributions of the two chemical branches cancel each other (Scheme 1). There are, however, in rigid matrix, additional mechanisms operational[15]: the three-spin mixing (TSM)[16,17] and the differential decay (DD)[18] mechanisms. These mechanisms require fulfillment of specific matching conditions depending, for example, on a particular architecture of spin states and a well-timed reaction kinetics as explored in magnetic field-dependent[19,3] and time-resolved[13,14] experiments. In RCs of *R. sphaeroides* (Figure SI3), the emissive intensity of the TSM dominates over the enhanced absorptive intensity of the DD leading to an entirely emissive spectral envelope[15,19]. As for the RPM, the TSM polarization is generated during inter-system crossing of the radical pair, coherently oscillating between

singlet and triple state. Therefore, RPM and TSM polarization are built up in parallel on the time-scale of the inter-system crossing frequency.

Combining isotope labeling with the solid-state photo-CIDNP effect appears to be an opportunity for combining two techniques to increase sensitivity and selectivity. In fact, selective ^{13}C isotope labeling of the tetrapyrrole cofactors allowed for atomic-scale insights into the electronic structure of the special pair donor in *Rhodobacter (R.) sphaeroides* in its electronic ground-state[20] as well as in its radical cation state[14]. Fully ^{13}C labeling at all carbon positions of the tetrapyrroles allowed analyzing the bacteriopheophytin acceptor cofactor and confirming that has no significant role in the functional symmetry break by the directed electron transfer[21]. With increase of label incorporation, it appeared that the effect of signal enhancement by the solid-state photo-CIDNP effect becomes weaker, in particular in steady-state experiments[21]. The reason for the loss of signal is not evident: it might be that the spin-dynamics producing the effect, which is presently only fully understood on the three-spin level, becomes 'disturbed' by the presence of further magnetic nuclei. Alternatively, it might be that the nuclear polarization occurs undisturbed but dissipates into the strongly coupled network of ^{13}C-^{13}C interactions. In an attempt to shed light on this question, we studied a fully labeled bacterial RC sample, entirely labeled at *all* ^{13}C and ^{15}N positions of protein and cofactors, by both continuous illumination as well as time-resolved photo-CIDNP MAS NMR techniques.

Materials and Methods

NMR experiments

NMR experiments were performed with a DMX-200 NMR spectrometer equipped with a double resonance CP/MAS probe (Bruker-Biospin, Karlsruhe, Germany). The sample was loaded into a clear 4-mm sapphire rotor and inserted into the MAS probe. The sample was frozen at a low spinning frequency of 1400 Hz to ensure a homogeneous sample distribution[22]. The light and dark spectra were collected using a Hahn echo pulse sequence with the CYCLOPS phase cycle of the (π/2) pulse. The data were collected with TPPM-15 carbon–proton decoupling[23] at a temperature of 222 K. The optimum length of the (π/2) carbon pulse, determined on uniformly ^{13}C labelled histidine, is ~ 6.3 μs at a strength of -3 dB. The rotational frequency for MAS was 8 kHz. For time-resolved measurements using a laser, both sequences in Figure SI1 had been used. No significant difference was observed in the spectra.

Lamp setup

The continuous illumination setup for the MAS NMR experiments comprises a xenon arc lamp (1000 W, Müller Elektronik-Optik) with collimation optics, a liquid filter and glass filters, a focusing element and a light fiber. Since the emission spectrum of a Xe lamp is similar to sunlight, the full range of radiation from UV to IR is available for illumination. Disturbance of the spinning frequency counting, which operates from a weak light source in the near-IR region, was avoided by a water filter as well as by various Schott filters such as WG320 and KG3. A fiber bundle was used to transfer the radiation from the collimation optics of the lamp to the sample[24,25].

Flash laser setup

Using 1064-nm flashes of a Nd:YAG laser (SpectraPhysics Quanta-Ray INDI 40-10, Irvine CA, USA), and frequency-doubling with a second harmonic generator, 532-nm laser flashes were generated with pulse length 6-8 ns and an energy between 20 to 270 mJ. The laser was operating with repetition frequencies between 15 Hz. The pump lamp of the laser was triggered by the triggering impulse from the spectrometer. The delay between the lamp trigger and the laser output (Q-switch mode) was measured to be 237 μs using a 500-MHz oscilloscope (Series TDS3000B, Tektronix, Beaverton, USA). Channel 1 of the oscilloscope and the lamp trigger channel (of the laser power-supply) were connected in parallel to the TTL channel of the spectrometer. Channel 2 of the oscilloscope was connected with the Q-switch sync (of the laser power supply). At the fiber output, the power of a laser pulse was ~ 50 mJ.

Optical coupling of laser and NMR

Radiation emitted by the laser is transferred to the sample via a fiber bundle (FiberTech GmbH, Berlin, Germany). A multi-mode light fiber bundle provides high optical transparency in a broad spectral range as well as sufficient mechanical flexibility for being attached to the stator of the MAS probe. The optically active diameter is 3 mm and the numerical aperture is 0.22. The ratio of the radiation energies between input and output powers of the fiber bundle is about 0.25. A Galilean lens system and a multi-mode fiber aligner are used for coupling the radiation pulses into the fiber bundle. The Galilean lens system, combining a concave lens with a convex one, allows collimation of the beam to the diameter required. The MAS NMR probe head (DMX-200, Bruker-Biospin GmbH, Karlsruhe, Germany) has been modified in order to illuminate the rotor from the side [24,25]. This includes (a) a bore drilled into the most upper partition plate separating stator chamber

and electronics, (b) drilling a small opening into the stator, and (c) winding a new coil from thin silver wire.

Sample preparation

Cultures of *R. sphaeroides* WT were grown anaerobically on synthetic Potnat medium containing 3g/L [U-^{13}C, ^{15}N] labelled algae hydrolysate. The cultures were allowed to grow for 7 days in light. For preparation of reaction centers, the culture was centrifuged for 10 minutes at 5500 × g and the pellet was re-suspended in 40 mL 0.1 M phosphate buffer (pH = 7.5). The RCs were isolated as described by Shochat *et al.* (1994)[26]. A protein/pigment ratio A_{280}/A_{802} = 1.2 was measured in the absorption spectrum to assess the purity of the samples. Approximately 5 mg of the RC protein complex embedded in LDAO micelles was used for NMR measurements. Prior to NMR experiment the RCs were reduced with 0.1 M sodium dithionite and was loaded into a clear 4-mm sapphire rotor.

The ^{13}C, ^{15}N-isotope enrichment of the BRC was measured by gas-chromatography and electron impact mass spectrometry (GC-MS). First the proteins in the sample were hydrolysed (Raap et al 1990)[27] followed by the derivatization of amino acids using the method of Husek (1991)[28]. The GC-MS was performed using a GC Chrompack 25 m fused silica column (CP-sil-5CB 0.25 mm id.; MS ITD 700, Finnigan MAT). Incorporation of [$^{13}C_6$,$^{15}N_3$] in RC complex was more than 90%.

Results and discussion

Continuous illumination. Spectrum 1A shows a ^{13}C MAS NMR spectrum of the fully labeled RC sample without illumination obtained at 4.7 T (200 MHz ^{1}H frequency). As expected, all signals are absorptive (positive), and a typical ^{13}C spectrum of a protein showing signals from aliphatic and aromatic carbons and a strong signal from the amide carbons is observed. This

spectrum has been obtained using a Hahn echo pulse sequence with the CYCLOPS phase cycle of the (π/2) pulse with a cycle delay of 2 seconds. Upon continuous illumination using the white light of a xenon lamp (Spectrum 1B), the envelope is modified over the entire spectral range. In particular, the peaks in the aromatic range are significantly reduced. A difference spectrum (Spectrum 1C), shows that all light-induced effects are emissive, showing the same features as observed in spectra of an u-^{13}C-ALA labeled sample under continuous illumination[21]. The slightly dispersive difference shape of the carbonyl signal probably originates from potential phase shifts by heating. There are, however, two significant differences to previous experiments: the lines are much broader and some of the sharp signals observed earlier do not appear in the present work. We conclude that the strong coupling network in the entirely isotope labeled sample causes both effects, and we assume that application of homonuclear (^{13}C-^{13}C) decoupling would improve the spectral quality significantly.

As expected for continuous-illumination experiments, the light-induced signals arise from the carbons forming the conjugated π-system where the TSM and DD mechanisms act most efficiently. The high density of carbon nuclear spins allows for spread of polarization to near-by aliphatic carbon atoms. The emissive signals, caused by the dominance of the TSM over the DD mechanism[19], might suggest the absence of a strong impact of the high ^{13}C concentration on the spin dynamics. At 4.7 T the photo-CIDNP generation has been shown to be very efficient in RCs of natural isotope abundance[3]. Furthermore, this allows for observable steady-state hyperpolarization in uniformly labelled samples. However, at 9.4 T production of hyperpolarization appears to be slower than its dissipation, and no hyperpolarization has been observed under continuous illumination (data not shown). These results demonstrate that the solid-state photo-CIDNP effect also occurs in quantitatively ^{13}C labeled samples; the results also show the occurrence of polarization transfer to near-by

aliphatic nuclei. The latter is presumably driven by spin-diffusion. For studying primary nuclear hyperpolarization prior to any secondary spin-diffusion processes occurring on millisecond time-scales, we employed laser-flash experiments for time-resolved generation of nuclear hyperpolarization[13].

The initial transient polarization. For observation of the original nuclear ^{13}C hyperpolarization build-up prior to spin-diffusion phenomena, we apply time-resolved excitation using nanosecond laser flashes for sample illumination (Figure S1)[13]. The spectrum showing the earliest transient polarization detected is presented in Figure 2. A set of some selected data obtained during the time evolution of are presented in Figure 3, and the full data set is shown in Figure SI2.

The two spectra shown in Figure 2 have been obtained with a delay period between light-flash and NMR detection of 0 μs. In a dark run (*i.e.*, no light flash), features of a typical protein spectrum appear with low intensity relative to the noise (Spectrum 2A). The low intensity of all signals is caused by pre-saturation, removing the entire Boltzmann polarization before the experiment. Hence, that the polarization observed directly after the light pulse is almost entirely photochemically induced. Spectrum 2B, obtained with a light flash at $\Delta = 0$ μs, shows strong light-induced signals throughout the spectrum: there are enhanced absorptive (positive) signals in the aliphatic (30-0 ppm) and the aromatic (180-140 ppm) regions, while emissive (negative) signals occur in the carbonylic (around 190 ppm) and the methinic (110-90 ppm) areas. Furthermore, emissive intensity dominates around 50 ppm, and between 130 and 110 ppm a mixed positive and negative pattern is observed. The observed pattern is well in-line with the expectations for RPM-induced nuclear polarization, depending on the sign and size of the isotropic hyperfine interaction (a_{iso})[14,29]. The emissive signals originate from carbons of the Special Pair donor for which negative values of the

isotropic hyperfine coupling to the aliphatic carbons (a_{iso}) have been calculated[14], such as C8, C17 and C18 with chemical shifts around 50 ppm (for carbon numbering, see Figure SI3), the methine carbons as well as the carbonylic carbons. The emissive signals at about 130 ppm can be assigned straightforwardly to C3. Solely the assignment of the emissive signal at about 120 ppm is not directly evident: the chemical shift would suggest an assignment to C12 for which a slight positive value has been calculated. Similarly, the assignment of the enhanced absorptive signals carbons for which positive values of a_{iso} have been predicted can be achieved. Carbons as C7[1] and C8[1] have chemicals shifts between 20 and 30 ppm and show large positive a_{iso} values. Clearly assigned carbons as C1, C6, C9, C11, C16 and C19 appear at chemical shifts between 145 and 170 ppm, have all been shown to possess positive a_{iso}-values. Hence, the initial kinetic phase of the time-resolved photo-CIDNP MAS NMR data reveals unequivocally the occurrence of RPM-induced nuclear polarization. In agreement to its sign pattern, this RPM polarization originates from the singlet channel[29].

Evolution of nuclear polarization. With increasing time-delay (Δ) between laser-flash and NMR detection, the spectral features change significantly (Figure 3). The initial RPM envelope (Spectra 2B and 3A) declines as indicated by the decay of the group of aliphatic signals at around 25 ppm. At the same time, on a microsecond timescale, emissive signals in the aromatic region become dominant (Spectra 3B and C). At 660 μs, the spectrum has only emissive signals in the aromatic region (Spectrum 3C). Hence, at that time, the RPM polarization has fully decayed and the polarization observed now arises from other sources. It is reasonable to assume that these sources are due to the TSM and DD mechanisms. TSM and DD have built up after the recombination, i.e., within some tens of ns. Both mechanisms contribute from early on but they are covered up by the dominant singlet channel RPM polarization which decays and reveals TSM and DD[13] displaying entirely emissive signals in *R. sphaeroides* WT RCs[19].

For the occurrence of spin-diffusion, as indicated by the emissive aliphatic signals observed under steady-state conditions in the continuous illumination experiment (Figure 1C), micro- and milliseconds are required. On a millisecond timescale, the emissive TSM envelope is significantly weakened but still visible. At 30 ms, as an example, a typical protein envelope occurs and only weak emissive signals of the previous states of hyperpolarization remain (Figure 3D). The main effect, however, is due to the build-up of the dark protein spectrum occurring with T_1 after the pre-saturation.

Kinetic analysis. The kinetics of the evolution of the signal intensity for selected signals is shown in Figure 4. The fitting parameters are summarized in Table S1. The decay kinetics of the enhanced absorptive aliphatic signals at 24 (line *f*), 28 (line *e*) and 31 (line *d*) ppm is solely linked to the decline of the RPM intensity. All three signals have decayed after about 500 µs. A global fit allows for a bi-exponential decay with time constants of $k_{d(RPM)1}$ = 145 µs and $k_{d(RPM)2}$ = 124 µs. These values are quite similar and might reflect the complexity of the radical pair dynamics. Also the decay of some emissive signals can be fitted well with the same kinetic parameter set: examples are the signals at 47 (line *c*), 107 (line *b*) and 119 (line *a*) ppm. The two aromatic signals, however, do not decay to zero but to values given by the emissive TSM intensity. In any case, the lifetime of the RPM polarization is remarkable long, significantly longer than the typical lifetime of the ^{3}Car state in a WT sample at natural abundance (5-10 µs). The lifetime is in the range of that of the carotenoid-less mutant R26 (100 µs)[13]. On the other hand, in R26 samples an additional differential relaxation mechanism (DR) occurs[30,31,3] but the present sample does not show any indication for such an effect. The absence of the DR might imply that not the lifetime of ^{3}P is extended but that of the ^{3}Car state. During lifetime of the ^{3}Car state, the nuclear polarization of the triplet decay branch has been shown to be hidden by the near-by paramagnet[13]. It might be that in the fully ^{13}C-

labelled Car, the coupling of vibrations to ISC is disturbed. Alternatively, the radical pair lifetimes might be extended.

The position at 164 ppm is particularly suited for kinetic analysis. Here, the initially enhanced absorptive signal due to RPM polarization decays and turns emissive by the TSM contributions (Figure 5 and Table S1). To allow a logarithmic scale to be used, some data points have been added showing the early evolution. It appears that the dynamics start after a delay period of about 30 µs. During that period, it might be that there is still continuous input from both decay channels of the radical pair, also implying a much longer radical pair lifetime than in samples at natural abundance. After 30 µs, a sharp decay occurs for which a kinetic constant of $k_{r(TSM)}$ = 5 µs has been found (Figure 6). That lifetime is a typical value for the ^{3}Car decay in natural abundance WT samples[13]. If that assignment would be correct, the nuclear polarization of the triplet branch might now become effective after the "drying up" of the spin-sorting radical pair. In any case, the isotope labeling has a significant effect on the kinetics of the triplet decay branch.

For the rise of the signal intensity towards equilibrium polarization, two steps have been resolved (Figure 5). In the period between 50 and 100 microseconds, the emissive polarization disappears largely but not entirely. The second step occurs on the timescale of hundreds of microseconds. While for the first step a kinetic constant of $k_{d1(TSM)}$ = 14 µs has been determined (Figure 7), the exact kinetic constant of the very slow second phase cannot be obtained on the basis of the present data. Since T_1 relaxation[24] as well as spin-spin J-coupling are significantly slower, we assign these two steps to spin-diffusion processes driven by homonuclear cross-relaxation. We assume that the fast process is caused by intramolecular equilibration of polarization occurring within the cofactors, while the slow process is the intermolecular polarization dissipation caused by the flow of polarization into

the protein matrix. If this assignment was right, there would be around 100 microseconds for keeping hyperpolarization confined on the cofactor, which is sufficiently long for many NMR experiments to explore the cofactor properties. The rather fast intramolecular equilibration process might be due to the slow MAS frequency and the strongly overlapping signals.

Conclusions. For the first time, an entirely $^{13}C^{15}N$-isotope enriched sample has been studied by solid-state photo-CINDP MAS NMR. Hyperpolarisation has been observed under continuous illumination as well as in microsecond time resolution using an 8 nanosecond laser flash. Hence, RPM as well as the solid-state mechanism TSM are active under high-label conditions proving that multiple labeling does not diminish the effect. It appears that the kinetics of the triplet decay branch is significantly altered upon increase of concentration of ^{13}C isotopes: (i) The lifetime of the RPM polarization is significantly extended and (ii) the arrival of the polarization from the triplet branch is remarkably delayed. Hyperpolarization is available on millisecond timescale allowing for application of more advanced pulse schemes. Application of homonuclear decoupling schemes might allow to control spin diffusion and to enhance signals in a larger area by so-called spin-torch experiments. Spin diffusion can be resolved into a fast intramolecular and a slow intermolecular kinetic phase. This result might also be relevant for the exploration for a possible ^{1}H photo-CIDNP solid-state effect in which nuclear interactions are even stronger.

ASSOCIATED CONTENT

Supporting Information. The fitting parameters, pulse sequences, the full data set obtained in the time-resolved experiment as well as the molecular structure of a BChl *a* and a BPheo *a* are provided. This material is available free of charge via the Internet at http://pubs.acs.org.

AUTHOR INFORMATION

Corresponding Author

*joerg.matysik@uni-leipzig.de. Fax: +49-341-9736115

Author Contributions

The manuscript was written through contributions of all authors. All authors have given approval to the final version of the manuscript.

Funding Sources

Financial support from the Netherlands Organisation for Scientific Research (NWO, 818.02.019) and the Deutsche Forschungsgemeinschaft (DFG, MA 497/2-1) is gratefully acknowledged.

ACKNOWLEDGMENT

This publication is dedicated to Prof. Wolfgang Lubitz on the occasion of his 65th birthday. The authors thank Dr. Eugenio Daviso, Dr. Karthick Babu Sai Sankar Gupta, Prof. Matthias Ernst and Prof. Gunnar Jeschke for exciting discussions. Technical support from Upasana Roy and Dr. Matthias Findeisen is gratefully acknowledged.

ABBREVIATIONS

DD, differential decay; DR, differential relaxation; MAS, magic-angle spinning; photo-CIDNP, photochemically induced dynamic nuclear polarization; RC, reaction center; RPM, radical-pair mechanism; TSM, three-spin mixing.

Insert Table of Contents Graphic and Synopsis Here.

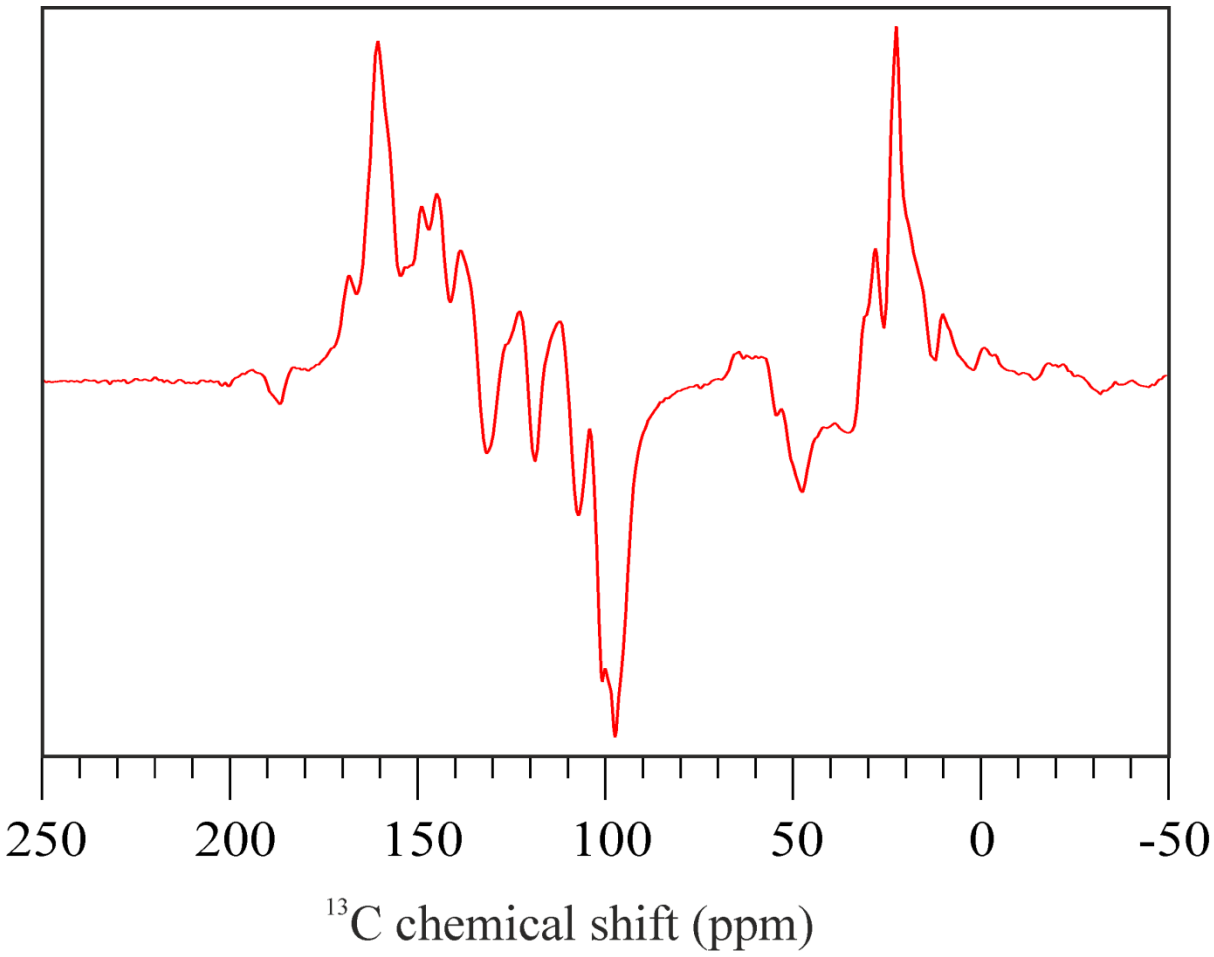

Synopsis: The solid-state photo-CIDNP effect occurs also in a fully ^{13}C and ^{15}N labeled reaction center protein.

Figures

Figure 1. ^{13}C photo-CIDNP MAS NMR spectra of u-^{13}C,^{15}N labeled *R. sphaeroides* WT obtained (A) in the dark, and (B) under continuous illumination in a magnetic field of 4.7 Tesla and at a temperature of 222 K. Spectrum (C) shows the difference (light - dark). The MAS frequency was 8 kHz.

Figure 2. ^{13}C time-resolved photo-CIDNP MAS NMR spectra of u-^{13}C,^{15}N labeled *R. sphaeroides* WT obtained (A) in the dark, and (B) immediately after laser flash using 532-nm 8-ns flashes (Δ = 0 μs). All the spectra have been recorded in a magnetic field of 4.7 Tesla and at a temperature of 222 K. The MAS frequency was 8 kHz.

Figure 3. ^{13}C time-resolved photo-CIDNP MAS NMR spectra of u-^{13}C,^{15}N labeled *R. sphaeroides* WT obtained with laser flash using 532-nm 8-ns flashes with four selected time delays (Δ) between the light pulse and the rf pulse: (A) 0 µs, (B) 50 µs, (C) 660 µs and (D) 30ms. All the spectra have been recorded in a magnetic field of 4.7 Tesla and at a temperature of 222 K. The MAS frequency was 8 kHz.

Figure 4. Normalized signal intensities plotted as a function of the delay-time Δ between the light pulse and the rf pulse for selected ^{13}C resonances from u-^{13}C,^{15}N labeled *R. sphaeroides* WT. For numbering and assignment of the carbons along with the fitting parameters, see Table S1.

Figure 5. Normalized intensities plotted as a function of the delay-time between the light pulse and the rf pulse for C-19 P_M from u-^{13}C,^{15}N labeled *R. sphaeroides* WT.

Figure 6. Normalized intensities plotted as a function of the delay-time between the light pulse and the rf pulse for C-19 P_M from u-^{13}C,^{15}N labeled *R. sphaeroides* WT.

This shows the decay of RPM with (arrival of magnetization for triplet branch partially overlapping the RPM pattern by TSM pattern) a time constant 5 ± 1 μs (from fitting). Details of the fitting is given in SI.

Figure 7. Normalized intensities plotted as a function of the delay-time between the light pulse and the rf pulse for C-19 P_M from u-^{13}C,^{15}N labeled *R. sphaeroides* WT. This shows the equilibration of TSM polarization with a time constant 14 ± 3 μs (from fitting). Details of the fitting is given in SI.

Scheme 1. Kinetics and spin dynamics of electron transport in quinone-depleted bacterial RCs of *R. sphaeroides* wild type (WT) at natural abundance. After absorption of a photon the photochemically excited state of the primary donor P* is formed and an electron is transferred to the primary acceptor ϕ_A, a bacteriopheophytin cofactor. Initially, the radical pair is in its singlet state $^1(P^{\bullet+}\Phi_A^{\bullet-})$. It evolves into a triplet state $^3(P^{\bullet+}\Phi_A^{\bullet-})$ due to the electron spin interactions and hyperfine coupling with nearby nuclei, a process which is known as intersystem crossing (ISC). The radical-pair mechanism (RPM) leads to sorting of nuclear spins via the isotropic hyperfine coupling, but without a net increase of the population difference of the spin up and the spin down nuclear states. In the TSM, hyperfine coupling, nuclear and electronic Zeeman interactions, and anisotropic interactions involving electrons and nuclei lead to symmetry breaking and net nuclear polarization that can be observed both in laser excitation experiments and under steady state conditions. The lifetime for recombination from the singlet state to the ground state is 20 ns, while charge recombination from the $^3(P^{\bullet+}\Phi_A^{\bullet-})$ radical pair state forms a donor triplet state ^3P with a time constant of 1 ns. With continuous illumination the difference in recombination rates from the singlet and triplet states to

the neutral ground state also break the symmetry when they match the inverse of the pseudosecular component of the hyperfine interaction, a process which is known as the DD mechanism. For the WT, the ^{3}P state is rapidly converted (100 ns) in a arotenoid triplet state (^{3}Car) and followed by a much slower decay from the carotenoid triplet state to the ground state (5-10 μs). A large fraction of the ^{3}P state decays via ^{3}Car, in competition with back conversion to the $^3(P^{\bullet+}\Phi_A^{\bullet-})$ radical pair. Time-resolved experiments have shown that during the ^{3}Car lifetime transient RPM polarization remains although the population of the triplet branch reached already the electronic ground state. Apparently, the strong electronic paramagnetism of ^{3}Car hides the nuclear spin polarization on the near-by P donor extending the visibility of the transient RPM polarization. After decay to the diamagnetic electronic ground state, the intensities of TSM and DD remain. If the ^{13}C concentration allows, these intensities equilibrate by spin diffusion. In samples with ^{13}C at natural abundance, the ^{13}C T_1 relaxation controls the decay of hyperpolarization.

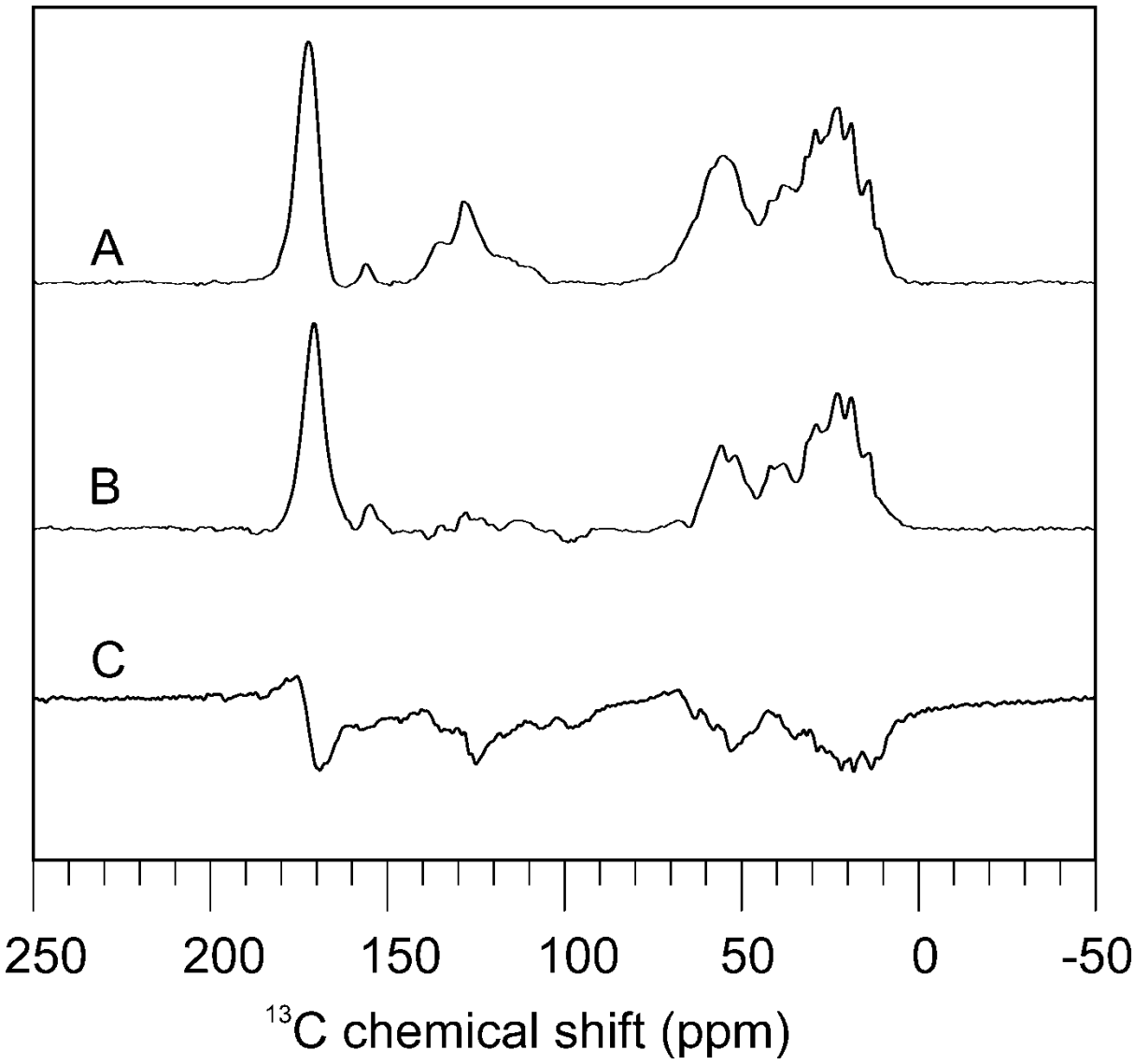

Figure 1.

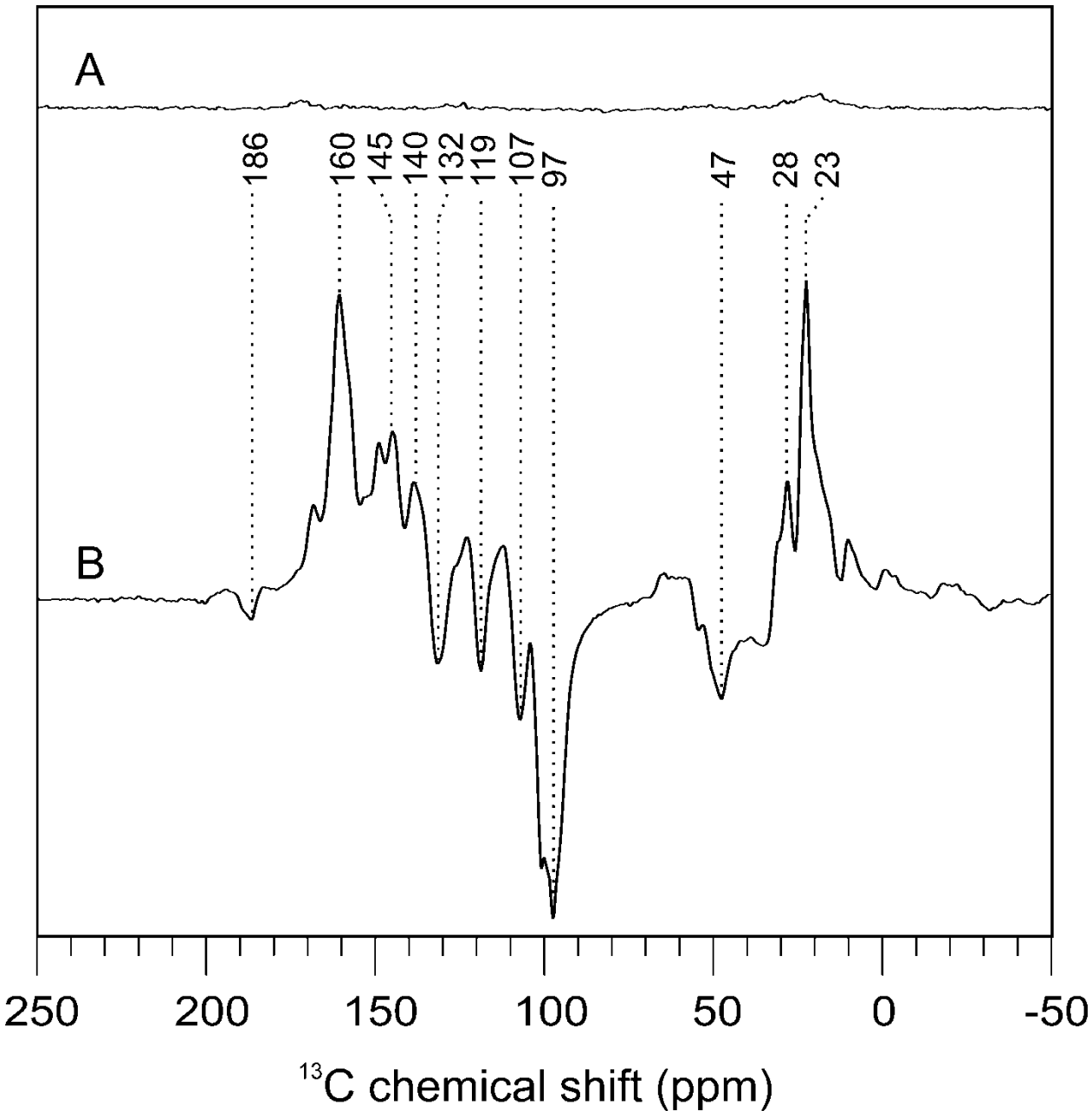
A
B
186
160
145
140
132
119
107
97
47
28
23
250
200
150
100
50
0
-50
13C chemical shift (ppm)

Figure 2.

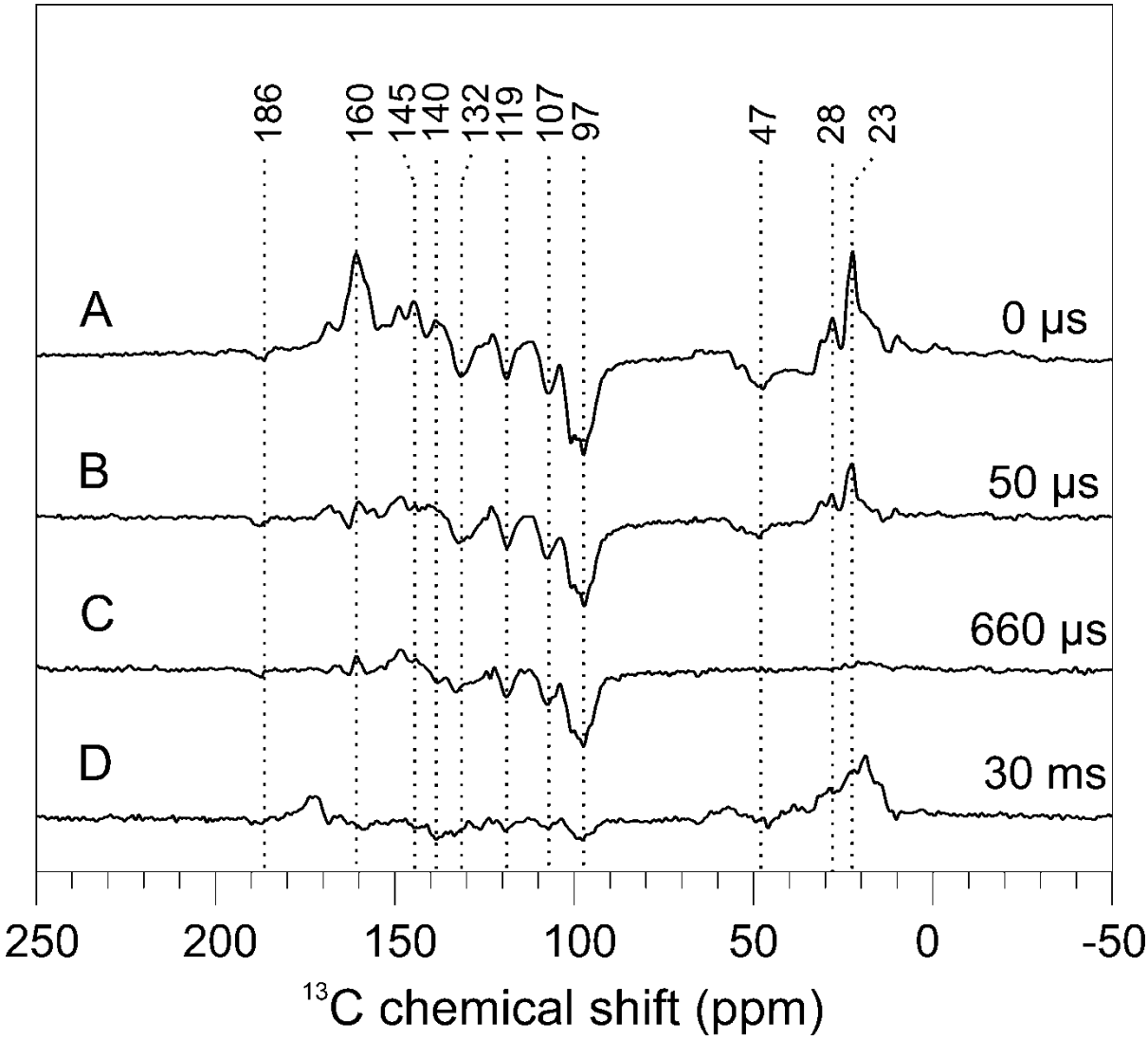
186
160
145
140
132
119
107
97
47
28
23
A
0 µs
B
50 µs
C
660 µs
D
30 ms
250
200
150
100
50
0
-50
13C chemical shift (ppm)

Figure 3.

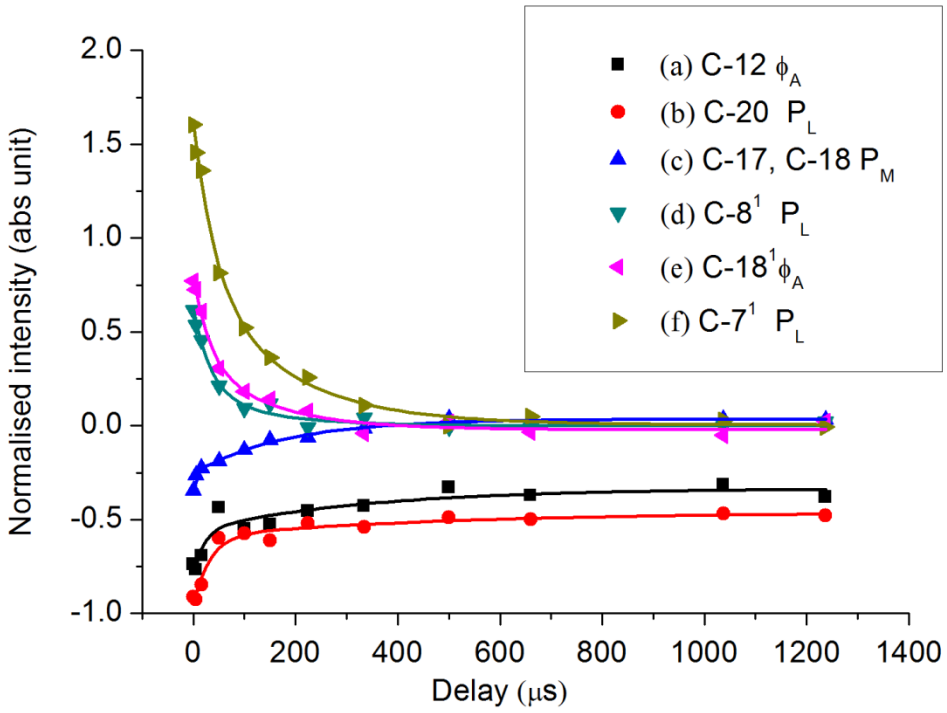
(a) C-12 ϕ_A
(b) C-20 P_L
(c) C-17, C-18 P_M
(d) C-8^1 P_L
(e) C-18$^1\phi_A$
(f) C-7^1 P_L
Normalised intensity (abs unit)
2.0
1.5
1.0
0.5
0.0
-0.5
-1.0
0
200
400
600
800
1000
1200
1400
Delay (μs)

Figure 4.

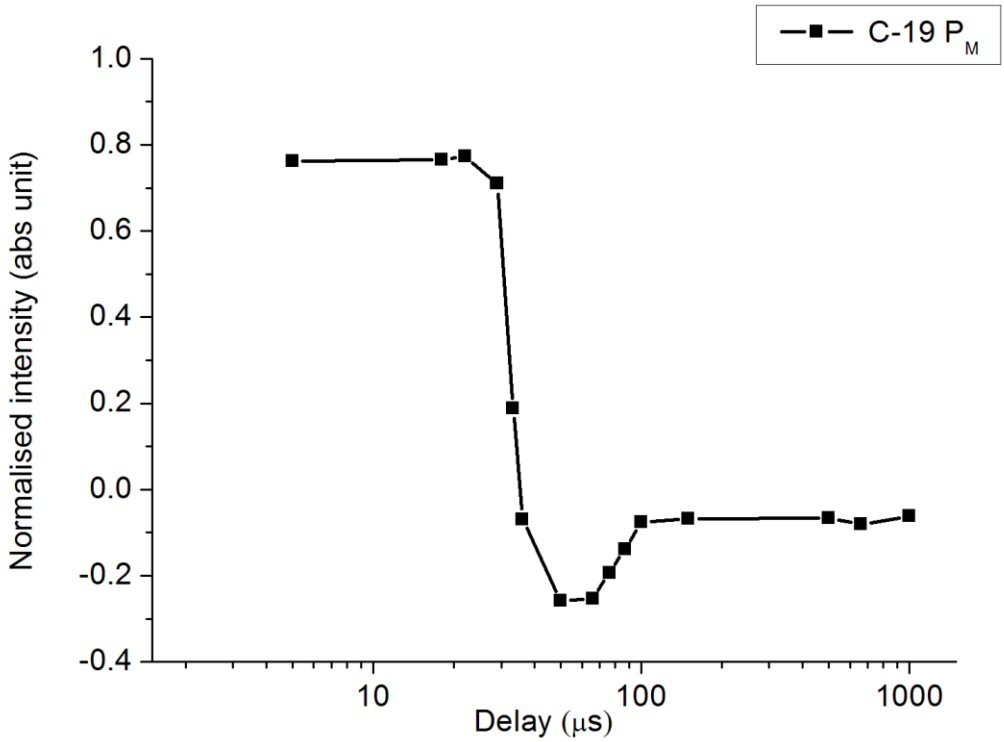
C-19 P M
Normalised intensity (abs unit)
1.0
0.8
0.6
0.4
0.2
0.0
-0.2
-0.4
10
100
1000
Delay (μs)

Figure 5.

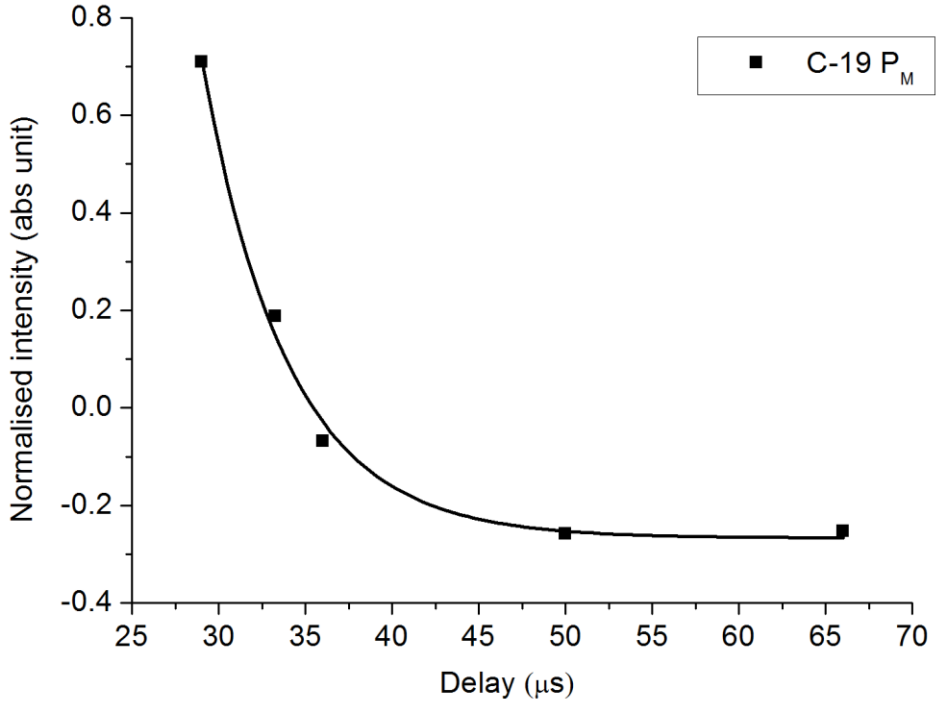
C-19 P_M
Normalised intensity (abs unit)
0.8
0.6
0.4
0.2
0.0
-0.2
-0.4
25
30
35
40
45
50
55
60
65
70
Delay (μs)

Figure 6.

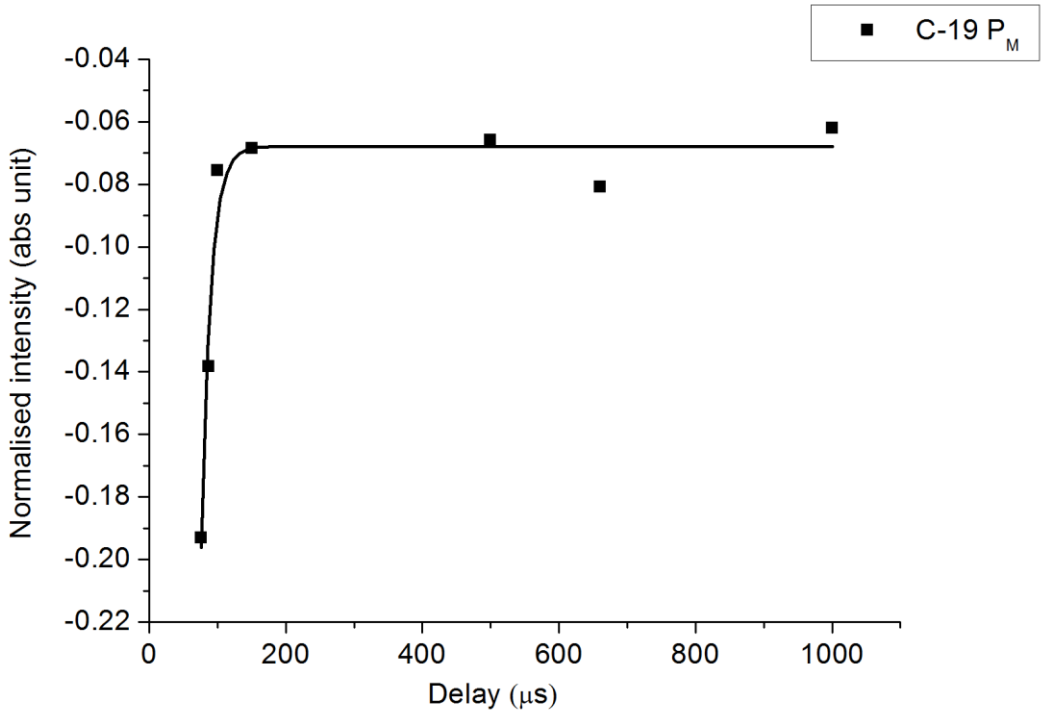
C-19 P_M
Normalised intensity (abs unit)
-0.04
-0.06
-0.08
-0.10
-0.12
-0.14
-0.16
-0.18
-0.20
-0.22
0
200
400
600
800
1000
Delay (μs)

Figure 7.

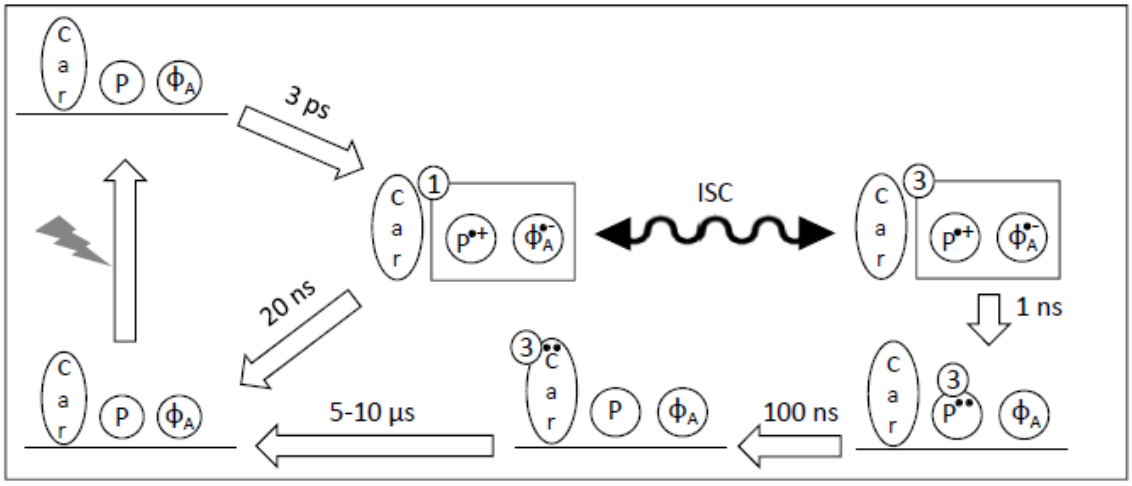

Scheme 1.

REFERENCES

1. Zysmilich, M. G.; McDermott, A., Photochemically Induced Dynamic Nuclear Polarization in the Solid-State 15N Spectra of Reaction Centers from Photosynthetic Bacteria Rhodobacter sphaeroides R-26. *J. Am. Chem. Soc.* **1994,** *116* (18), 8362-8363.
2. Bode, B.; Thamarath, S.; Gupta, K.; Alia, A.; Jeschke, G.; Matysik, J., The Solid-State Photo-CIDNP Effect and Its Analytical Application. In *Hyperpolarization Methods in NMR Spectroscopy*, Kuhn, L. T., Ed. Springer Berlin Heidelberg: 2013; Vol. 338, pp 105-121.
3. Thamarath, S. S.; Bode, B. E.; Prakash, S.; Sai Sankar Gupta, K. B.; Alia, A.; Jeschke, G.; Matysik, J., Electron Spin Density Distribution in the Special Pair Triplet of Rhodobacter sphaeroides R26 Revealed by Magnetic Field Dependence of the Solid-State Photo-CIDNP Effect. *J. Am. Chem. Soc.* **2012,** *134* (13), 5921-5930.
4. Diller, A.; Roy, E.; Gast, P.; van Gorkom, H. J.; de Groot, H. J. M.; Glaubitz, C.; Jeschke, G.; Matysik, J.; Alia, A., 15N photochemically induced dynamic nuclear polarization magic-angle spinning NMR analysis of the electron donor of photosystem II. *Proceedings of the National Academy of Sciences* **2007,** *104* (31), 12767-12771.
5. Roy, E.; Rohmer, T.; Gast, P.; Jeschke, G.; Alia, A.; Matysik, J., Characterization of the Primary Radical Pair in Reaction Centers of Heliobacillus mobilis by 13C Photo-CIDNP MAS NMR†. *Biochemistry* **2008,** *47* (16), 4629-4635.
6. Roy, E.; Alia; Gast, P.; van Gorkom, H.; de Groot, H. J. M.; Jeschke, G.; Matysik, J., Photochemically induced dynamic nuclear polarization in the reaction center of the green sulphur bacterium Chlorobium tepidum observed by 13C MAS NMR. *Biochimica et Biophysica Acta (BBA) - Bioenergetics* **2007,** *1767* (6), 610-615.
7. Janssen, G.; Daviso, E.; van Son, M.; de Groot, H. M.; Alia, A.; Matysik, J., Observation of the solid-state photo-CIDNP effect in entire cells of cyanobacteria Synechocystis. *Photosynth Res* **2010,** *104* (2-3), 275-282.
8. Wang Xiaojie, S. S. T., J; #246; Matysik, r., Magnetic Field Dependence of the Solid-State Photo-CIDNP Effect Observed in Phototropin LOV1-C57S. *Acta Chim. Sinica* **2013,** *71* (02), 169-172.
9. Thamarath, S. S.; Heberle, J.; Hore, P. J.; Kottke, T.; Matysik, J., Solid-State Photo-CIDNP Effect Observed in Phototropin LOV1-C57S by 13C Magic-Angle Spinning NMR Spectroscopy. *J. Am. Chem. Soc.* **2010,** *132* (44), 15542-15543.
10. Matysik, J.; Diller, A.; Roy, E.; Alia, A., The solid-state photo-CIDNP effect. *Photosynth Res* **2009,** *102* (2-3), 427-435.
11. Closs, G. L.; Closs, L. E., Induced dynamic nuclear spin polarization in reactions of photochemically and thermally generated triplet diphenylmethylene. *J. Am. Chem. Soc.* **1969,** *91* (16), 4549-4550.
12. Kaptein, R.; Oosterhoff, J. L., Chemically induced dynamic nuclear polarization II: (Relation with anomalous ESR spectra). *Chemical Physics Letters* **1969,** *4* (4), 195-197.
13. Daviso, E.; Alia, A.; Prakash, S.; Diller, A.; Gast, P.; Lugtenburg, J.; Matysik, J.; Jeschke, G., Electron−Nuclear Spin Dynamics in a Bacterial Photosynthetic Reaction Center. *The Journal of Physical Chemistry C* **2009,** *113* (23), 10269-10278.
14. Daviso, E.; Prakash, S.; Alia, A.; Gast, P.; Neugebauer, J.; Jeschke, G.; Matysik, J., The electronic structure of the primary electron donor of reaction centers of purple bacteria at atomic resolution as observed by photo-CIDNP 13C NMR. *Proceedings of the National Academy of Sciences* **2009,** *106* (52), 22281-22286.

15. Jeschke, G.; Matysik, J., A reassessment of the origin of photochemically induced dynamic nuclear polarization effects in solids. *Chemical Physics* **2003,** *294* (3), 239-255.
16. Jeschke, G., A New Mechanism for Chemically Induced Dynamic Nuclear Polarization in the Solid State. *J. Am. Chem. Soc.* **1998,** *120* (18), 4425-4429.
17. Jeschke, G., Electron–electron–nuclear three-spin mixing in spin-correlated radical pairs. *The Journal of Chemical Physics* **1997,** *106* (24), 10072-10086.
18. Polenova, T.; McDermott, A. E., A Coherent Mixing Mechanism Explains the Photoinduced Nuclear Polarization in Photosynthetic Reaction Centers. *The Journal of Physical Chemistry B* **1999,** *103* (3), 535-548.
19. Prakash, S.; Alia; Gast, P.; de Groot, H. J. M.; Jeschke, G.; Matysik, J., Magnetic Field Dependence of Photo-CIDNP MAS NMR on Photosynthetic Reaction Centers of Rhodobacter sphaeroides WT. *J. Am. Chem. Soc.* **2005,** *127* (41), 14290-14298.
20. Schulten, E. A. M.; Matysik, J.; Alia; Kiihne, S.; Raap, J.; Lugtenburg, J.; Gast, P.; Hoff, A. J.; de Groot, H. J. M., 13C MAS NMR and Photo-CIDNP Reveal a Pronounced Asymmetry in the Electronic Ground State of the Special Pair of Rhodobacter sphaeroides Reaction Centers†. *Biochemistry* **2002,** *41* (27), 8708-8717.
21. Sai Sankar Gupta, K. B.; Alia, A.; Buda, F.; de Groot, H. J. M.; Matysik, J., Bacteriopheophytin a in the Active Branch of the Reaction Center of Rhodobacter sphaeroides Is Not Disturbed by the Protein Matrix as Shown by 13C Photo-CIDNP MAS NMR. *The Journal of Physical Chemistry B* **2013,** *117* (12), 3287-3297.
22. Fischer, M. R.; De Groot, H. J. M.; Raap, J.; Winkel, C.; Hoff, A. J.; Lugtenburg, J., Carbon-13 magic angle spinning NMR study of the light-induced and temperature-dependent changes in Rhodobacter sphaeroides R26 reaction centers enriched in [4'-13C]tyrosine. *Biochemistry* **1992,** *31* (45), 11038-11049.
23. Bennett, A. E.; Rienstra, C. M.; Auger, M.; Lakshmi, K. V.; Griffin, R. G., Heteronuclear decoupling in rotating solids. *The Journal of Chemical Physics* **1995,** *103* (16), 6951-6958.
24. Daviso, E.; Jeschke, G.; Matysik, J., Photochemically Induced Dynamic Nuclear Polarization (Photo-CIDNP) Magic-Angle Spinning NMR. In *Biophysical Techniques in Photosynthesis*, Aartsma, T.; Matysik, J., Eds. Springer Netherlands: 2008; Vol. 26, pp 385-399.
25. Matysik, J.; Alia; Hollander, J. G.; Egorova-Zachernyuk, T.; Gast, P.; De Groot, H. J. M., A set-up to study photochemically induced dynamic nuclear polarization in photosynthetic reaction centres by solid-state NMR. *Indian Journal of Biochemistry and Biophysics* **2000,** *37* (6), 418-423.
26. Shochat, S.; Arlt, T.; Francke, C.; Gast, P.; van Noort, P.; Otte, S. M.; Schelvis, H. M.; Schmidt, S.; Vijgenboom, E.; Vrieze, J.; Zinth, W.; Hoff, A., Spectroscopic characterization of reaction centers of the (M)Y210W mutant of the photosynthetic bacterium Rhodobacter sphaeroides. *Photosynth Res* **1994,** *40* (1), 55-66.
27. Raap, J.; Winkel, C.; de Wit, A. H. M.; van Houten, A. H. H.; Hoff, A. J.; Lugtenburg, J., Mass spectrometric determination of isotopically labeled tyrosines and tryptophans in photosynthetic reaction centers of Rhodobacter sphaeroides R-26. *Analytical Biochemistry* **1990,** *191* (1), 9-15.
28. Hušek, P., Rapid derivatization and gas chromatographic determination of amino acids. *Journal of Chromatography A* **1991,** *552* (0), 289-299.

29. Kaptein, R., Simple rules for chemically induced dynamic nuclear polarization. *Journal of the Chemical Society D: Chemical Communications* **1971,** (14), 732-733.
30. McDermott, A.; Zysmilich, M. n. G.; Polenova, T., Solid state NMR studies of photoinduced polarization in photosynthetic reaction centers: mechanism and simulations. *Solid State Nuclear Magnetic Resonance* **1998,** *11* (1–2), 21-47.
31. Prakash, S.; Alia; Gast, P.; de Groot, H. J. M.; Matysik, J.; Jeschke, G., Photo-CIDNP MAS NMR in Intact Cells of Rhodobacter sphaeroides R26: Molecular and Atomic Resolution at Nanomolar Concentration. *J. Am. Chem. Soc.* **2006,** *128* (39), 12794-12799.